Supplementary Figures

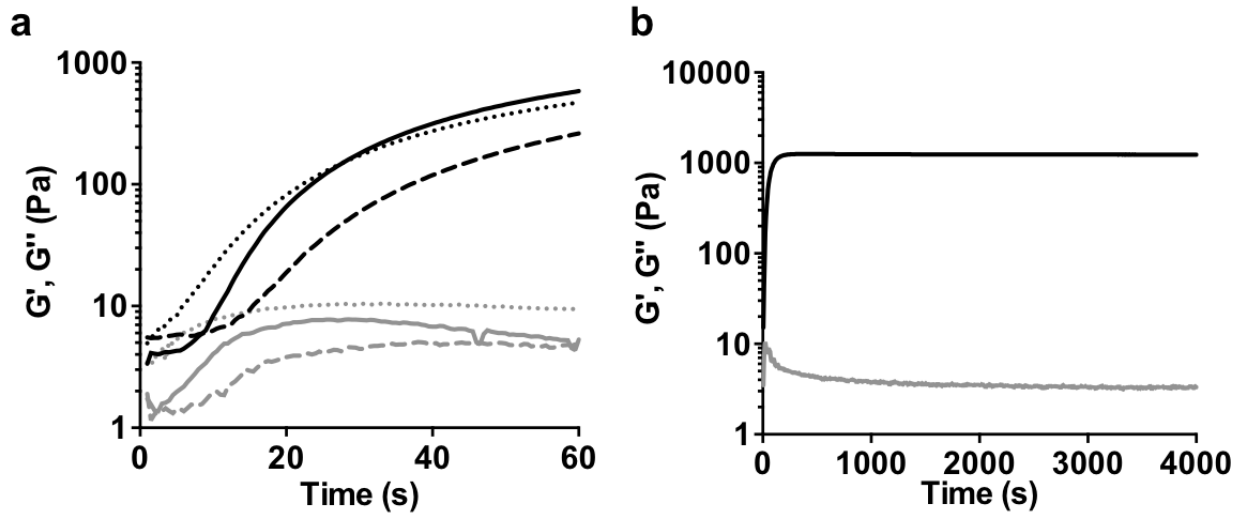

Figure S1. Network formation of allyl sulfide hydrogels. **a** The evolution of shear storage (black) and loss (gray) moduli are monitored with shear rheology for AS-PA (solid line), AS-AA (dotted), and AS-PhAA (dashed) crosslinkers. Crossover between the storage and loss moduli occur within 30s of mixing precursor solutions. **b** The evolution of shear storage (black) and loss (gray) moduli are monitored with shear rheology for an AS-PA crosslinked hydrogel. Following a plateau, the storage modulus remains constant.

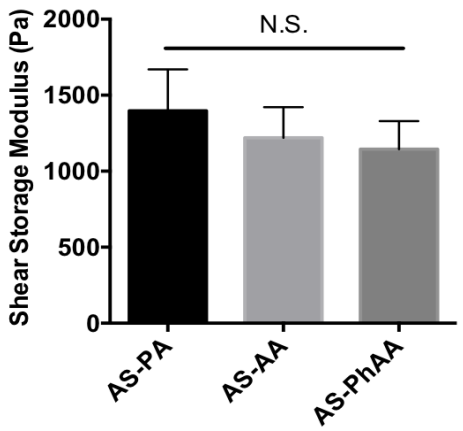

Figure S2. Equilibrated storage moduli of allyl sulfide hydrogels. The final equilibrated storage moduli of allyl sulfide hydrogels formed with AS-PA, AS-AA, and AS-PhAA hydrogels are statistically similar. Significance determined by one-way ANOVA, N=7, mean ± s.d..

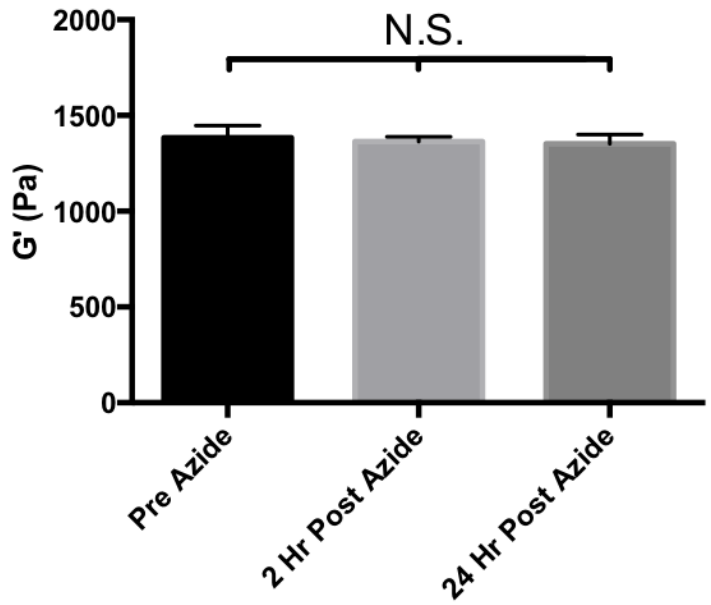

Figure S3 Time course of storage moduli for allyl sulfide hydrogels. The storage modulus of allyl sulfide hydrogels before the addition of PEG_3-N_3 (black) does not change after 2 hours (light grey) or 24 hours (dark grey) of equilibration. Significance determined by one-way ANOVA, N=3, mean ± s.d..

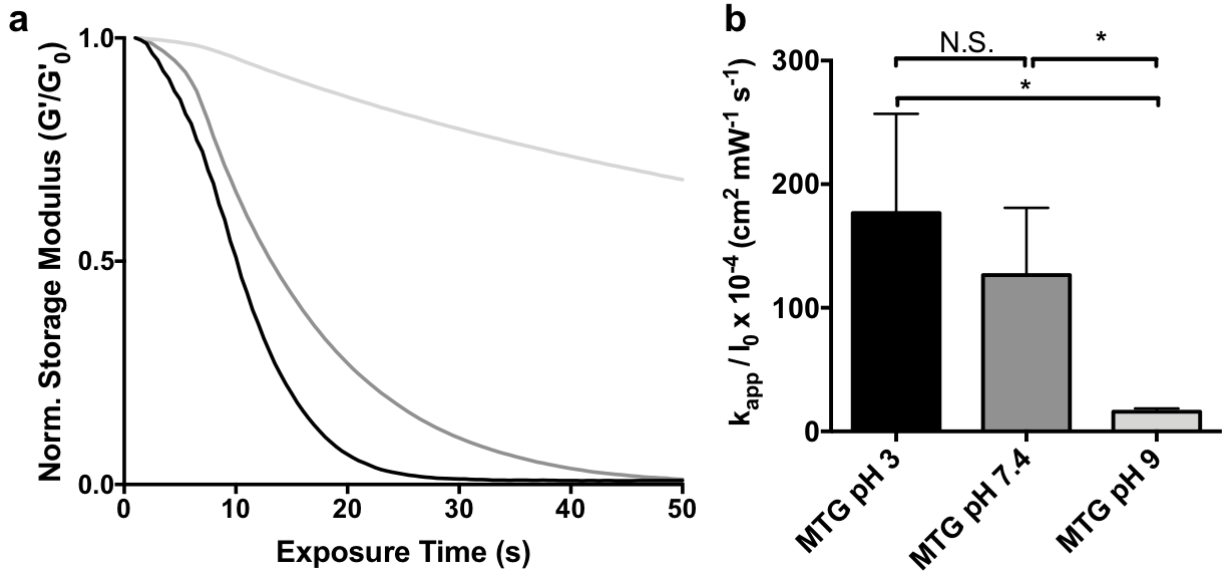

Figure S4. **a** The effect of solution pH on allyl sulfide degradation. AS-PA hydrogels were equilibrated with solutions of MTG at pH values of 3 (black), 7.4 (grey), and 9 (light grey) and degraded while tracking the shear storage modulus. The increasing solution pH generates more thiolate anions which participate in the formation of DRAs, hindering the degradation process. Rheological plot shows a representative trace from N=3. **b** Apparent rate constants for photodegradation of AS-PA using MTG at pH 3, pH 7.4 and pH 9 are shown. Significance determined by one-way ANOVA, N=3, mean ± s.d., *$p < 0.05$.

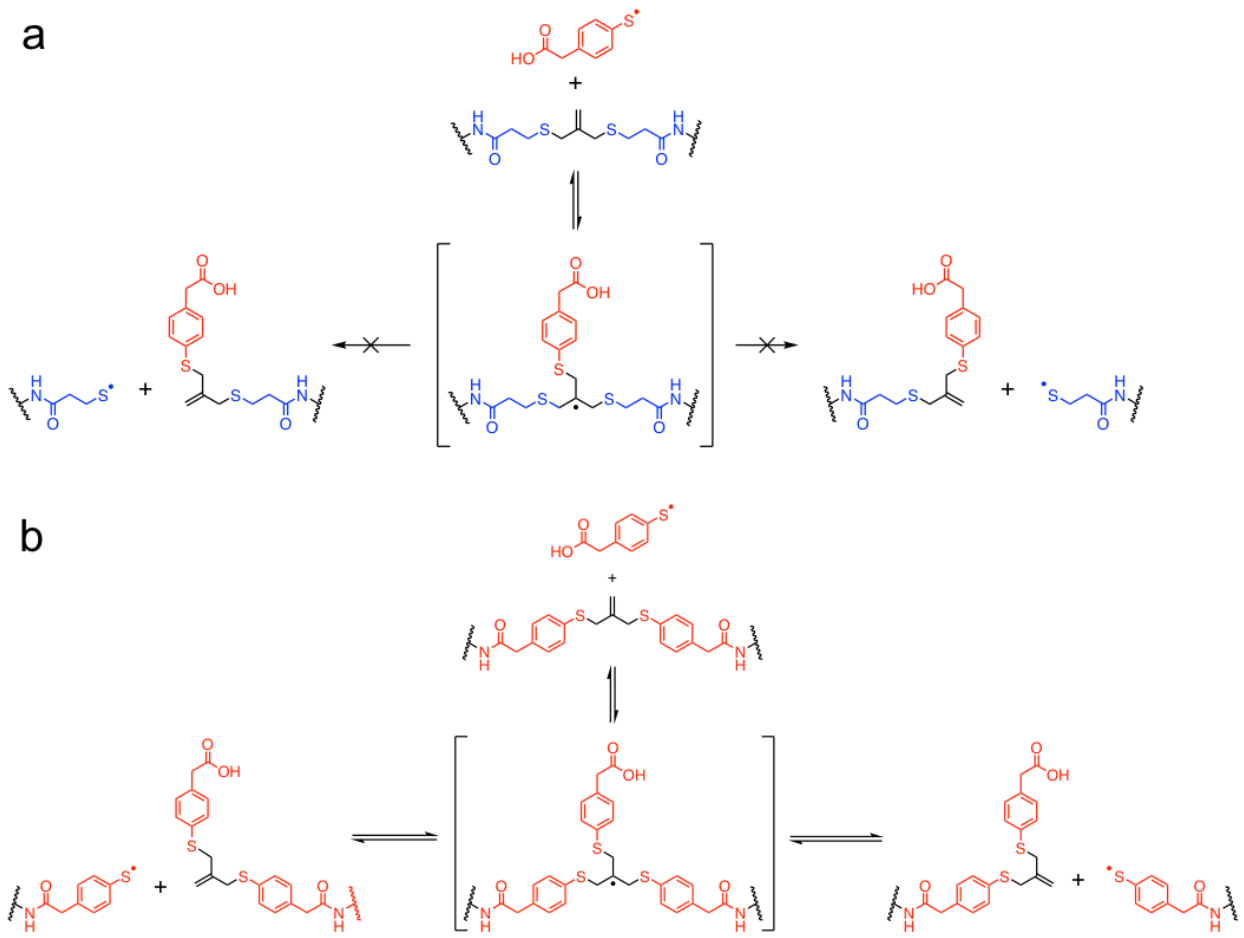

Figure S5. Degradation products of allyl sulfide crosslinkers with 4MPAA. **a** The reaction of AS-PA with 4MPAA results in the formation of an asymmetrical intermediate that favors the re-formation of the more stable aromatic thiyl radical. **b** The reaction of AS-PhAA with 4MPAA results in the formation of a symmetrical intermediate that has no favored degradation product, according to radical stability, allowing for photodegradation.

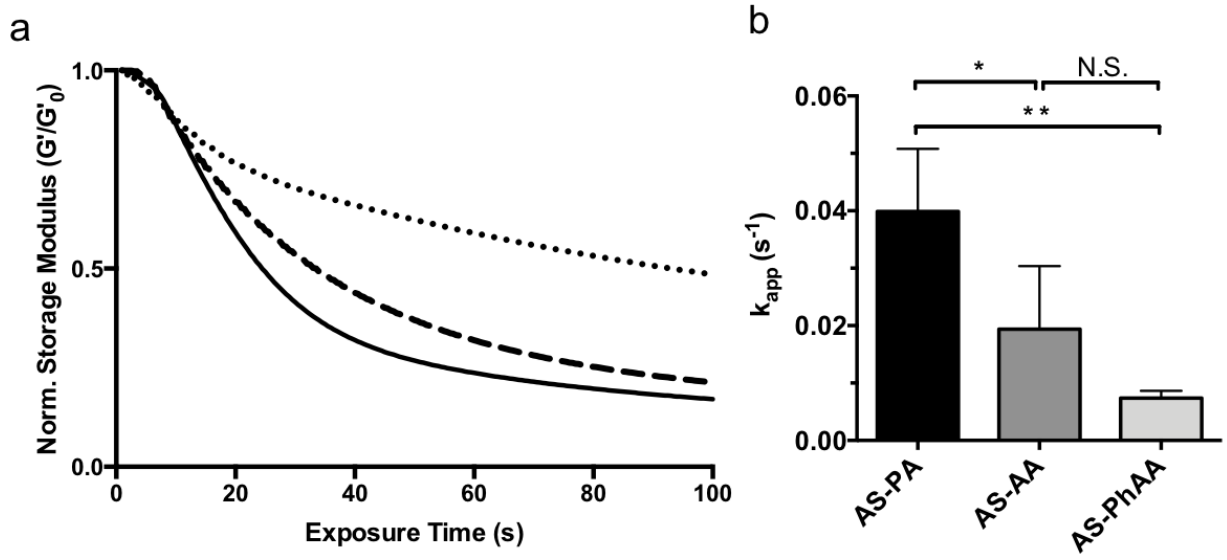

Figure S6. Allyl sulfide degradation due to initiator generated radicals. Hydrogels crosslinked with AS-PA (solid), AS-AA (dashed), and AS-PhAA (dotted), were degraded in the absence of thiol. Degradation is due to the irreversible addition of initiator generated radicals that cause cleavage of allyl sulfide crosslinks. Rheological plot shows a representative trace from N=3. **b** Apparent rate constants for photodegradation of AS-PA, AS-AA, and AS-PhAA crosslinked hydrogels using 1 mM LAP (no thiol) are shown. Significance determined by one-way ANOVA, N=3, mean ± s.d., *$p < 0.05$, **$p<0.01$

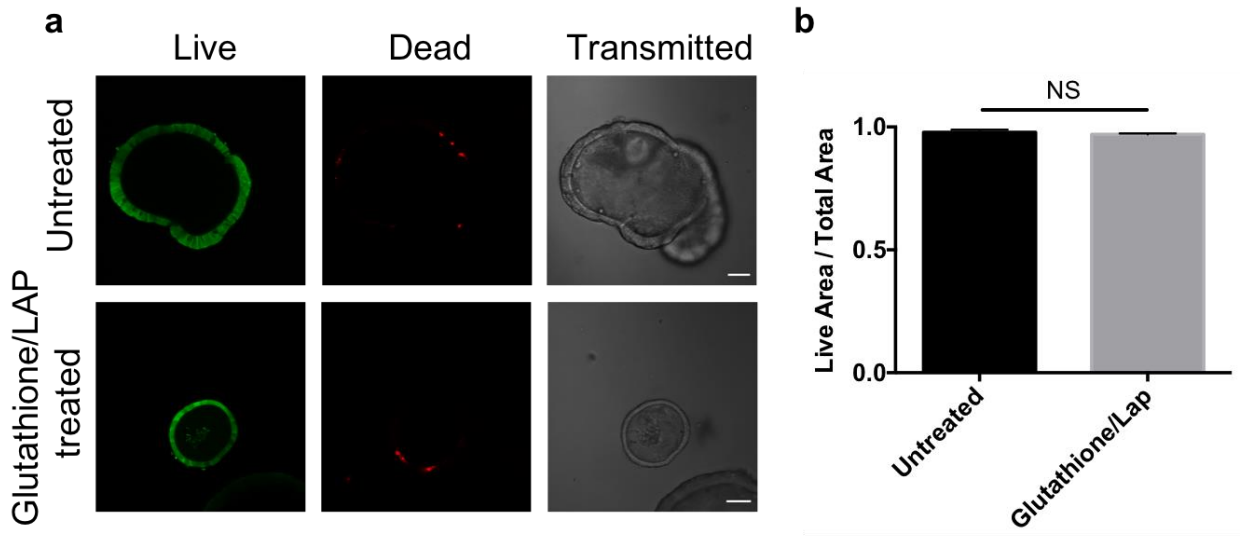

Figure S7. Viability of intestinal organoids following exposure to GSH and LAP. **a** Organoid growing in Matrigel were equilibrated with GSH (15×10^{-3} m) and LAP (1×10^{-3} m) for 30 minutes and subsequently stained with calcein-AM (live, green) and ethidium homodimer (dead, red). **b** Viability determined as the ratio of live stain area to total stain area (live + dead). Significance determined by one-way ANOVA, N=30, mean ± s.d.,

Supplementary Table

Extended Data Table 1. Sequence of Quantitative Real-Time PCR Primers

Real-Time Primers	Sequences (5’ to 3’)
CHGA-F	5'-AAGAAGAGGAGGAGGAAGAGG-3'
CHGA-R	5'-TCCATCCACTGCCTGAGAG-3'
DCLK1-F	5’-TCCACCGGAATTGAACTCGG-3’
DCLK1-R	5’-GGGAGCGAACAGTCTCAGA-3’
GapDH-F	5’-TATTATGGGGGTCTGGGATGG-3’
GapDH-R	5’-TCAAGAAGGTGGTGAAGCAGG-3’
Lactase-F	5'-CAGCGATGCCCACAGGAAAG-3'
Lactase-R	5'-ACGGAGCCCTTGACGAGA G-3'
Lgr5-F	5’-AGGCTGCCAAAAACTTCAGA-3’
Lgr5-R	5’-AGGGAAGGACGACAGGAGAT-3’
Lyz1-F	5’-GTGCCTGTCCTGATCTTTCT-3’
Lyz1-R	5’-GATTTGCTCCTGTGGTTATTGG-3’
Muc2-F	5'-AGAACGATGCCTACACCAAG-3'
Muc2-R	5'-CATTGAAGTCCCCGCAGAG-3'